local stability at the equilibrium point as its corresponding linear PI control system. Nevertheless, the behavior of these two systems can be quite different, as exemplified by the simulation results involving systems (3.16) and (3.17). Take system (3.17), for example. If one chooses such parameter values that make the PI control system barely stable, the corresponding fuzzy PI control system will probably oscillate fairly wildly before settling at the equilibrium point, resulting in a performance inferior to the PI system. After all, the overall equivalent gains of the fuzzy PI controller are larger than those of the linear PI controller. These parameter values are extreme for the fuzzy PI controller and thus should be excluded to make comparison fairer.

Conceptually, no controller of any type, conventional or fuzzy, can always outperform a controller of another type for all possible parameter settings. Thus, fairly and convincingly comparing two different types of controllers is tricky. In our case, it is fortunate that the structure of the fuzzy PI controller can be derived and that its relationship with the linear PI controller is established. These pave a way for making the fair comparisons between the fuzzy and linear PI controllers and for understanding the reasons behind the comparison outcome. We can confidently conclude that the fuzzy PI controllers, as nonlinear controllers, can outperform their linear counterparts when controlling nonlinear systems or systems with time delay.

3.8.4. Superior Fuzzy Control Performance at a Price

Better performance of the fuzzy PI controller comes with a price: Their structure is more complicated, and the number of adjustable parameters is larger. These characteristics cause the fuzzy controller to have more degrees of freedom in controller structure and parameters. The linear PI controller is very simple in structure and has only two tunable gains. The structure of the fuzzy PI controller is more complicated and has five adjustable parameters, namely, H, L, K_e, K_r, and $K_{\Delta u}$. As H and $K_{\Delta u}$ always appear as the product of $K_{\Delta u} \cdot H$ in the expressions (see Table 3.5, for instance), only one of them is an independent parameter. Without loss of generality, one can always assume that $H = L$. This still leaves four tunable parameters, and the parameter tuning is significantly more difficult than that for the linear PI controller.

3.9. SIMPLEST FUZZY PI CONTROLLERS USING DIFFERENT FUZZY INFERENCE METHODS

3.9.1. Configurations of Fuzzy PI Controllers

In this section, we study the analytical structure of the simplest fuzzy PI controllers that use the four different inference methods: The Mamdani minimum inference method, the Larsen product inference method, the drastic product inference method, and the bounded product inference method (Table 1.1). Recall that the different inference methods are meaningful only when the output fuzzy sets are not of the singleton type. Thus, the fuzzy controllers in this section use the three trapezoidal output fuzzy sets shown in Fig. 3.14. The other components of the fuzzy controllers are exactly the same as the fuzzy PI controllers above (i.e., two input fuzzy sets, four control rules, Zadeh fuzzy AND operator, Lukasiewicz fuzzy OR operator, and centroid defuzzifier). We now prove them to be different nonlinear PI controllers with variable proportional-gain and integral-gain.

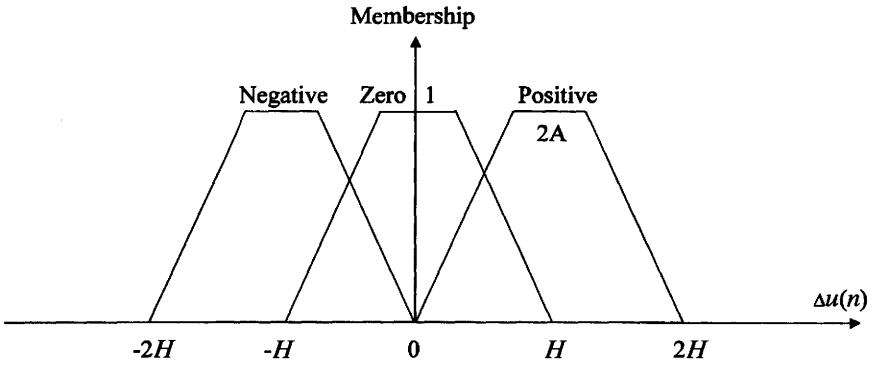

Figure 3.14 Three trapezoidal output fuzzy sets for the simplest nonlinear fuzzy PI controllers using the four different inference methods.

In Fig. 3.14, $2A$ and $2H$ are the upper and lower sides of the three trapezoidal fuzzy sets, respectively. Also, $-H$, 0, and H are the centers of Negative, Zero, and Positive fuzzy sets, respectively. To define the trapezoids, we introduce a parameter

$$\theta = \frac{A}{H}$$

and constrain it by

$$\theta \leq 0.5$$

to avoid overlay between the upper sides of two adjacent fuzzy sets.

3.9.2. Derivation and Resulting Structures

In our case, μ in Table 1.1 is the membership value for the output fuzzy set in each of the four fuzzy rules r1 to r4. The shadow areas in Fig. 3.15 represent the results of applying the four different inference methods to the trapezoidal output fuzzy sets. The formulas for computing the areas are given in Table 3.6. As in Table 1.1, the subscripts M, L, DP, and BP denote the four different inference methods. For rules r1 and r4, μ is μ_{r1} and μ_{r4}, respectively, whereas for rules r2 and r3, μ is $\mu_{r2\cup r3}$. We use the Zadeh fuzzy AND operator to compute μ_{r1} to μ_{r4}, and we use the Lukasiewicz fuzzy OR operator to calculate $\mu_{r2\cup r3}$ from μ_{r2} and μ_{r3}. After the centroid defuzzifier is applied, the incremental output of the fuzzy PI controllers is:

$$\begin{aligned}\Delta U(n) &= K_{\Delta u}\frac{S(\mu_{r1})H + S(\mu_{r2\cup r3}) \times 0 + S(\mu_{r4})(-H)}{S(\mu_{r1}) + S(\mu_{r2\cup r3}) + S(\mu_{r4})} \\ &= K_{\Delta u}H\frac{S(\mu_{r1}) - S(\mu_{r4})}{S(\mu_{r1}) + S(\mu_{r2\cup r3}) + S(\mu_{r4})},\end{aligned} \tag{3.18}$$

where $S(\mu_{r1})$ and $S(\mu_{r4})$, calculated according to Table 3.6, are the areas of the trapezoidal output sets Positive and Negative with the respective membership values, μ_{r1} and μ_{r4}. $S(\mu_{r2\cup r3})$ is the area of the trapezoidal output fuzzy set Zero, generated by the rules r2 and r3, with the combined membership value $\mu_{r2\cup r3}$.

The results of the Zadeh fuzzy AND operation in each of the four fuzzy rules are available (Table 3.1). The outcome of applying the Lukasiewicz fuzzy OR operator to the

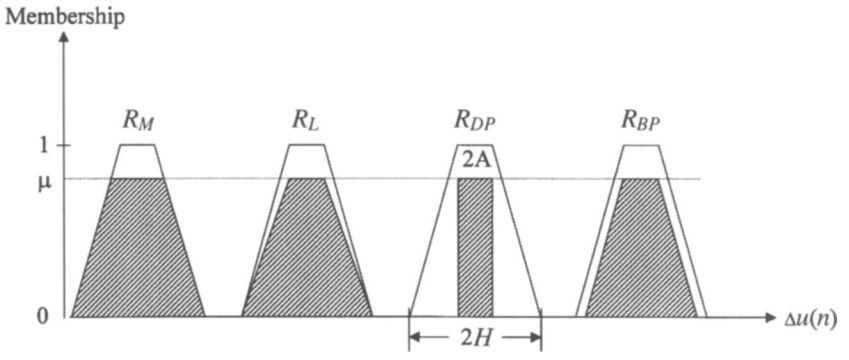

Figure 3.15 Fuzzy inference results: Shadow areas representing the results of applying the four different inference methods to the trapezoidal output fuzzy sets.

fuzzy rules r2 and r3 is simply the summation of the respective membership values (i.e., $\mu_{r2\cup r3} = \mu_{r2} + \mu_{r3}$). Replacing μ in Table 3.6 by μ_{r1}, $\mu_{r2\cup r3}$, and μ_{r4} and substituting the results into (3.18), analytical structures of the fuzzy PI controllers are obtained: They are nonlinear PI controllers with variable gains and can be described in general by

$$\Delta U(n) = K_i(e,r)e(n) + K_p(e,r)r(n),$$

where

$$K_p(e,r) = \beta(e,r)K_p(0,0) \quad \text{and} \quad K_i(e,r) = \beta(e,r)K_i(0,0).$$

For different inference methods, $\beta(e,r)$, $K_p(0,0)$), and $K_i(0,0)$ are different. We use the same notations as above for the inference methods, and we list four different $\beta(e,r)$ in Table 3.7 and $K_p(0,0)$ and $K_i(0,0)$ in Table 3.8 for IC1 to IC4.

The structure of the fuzzy controllers when either $E(n)$ or $R(n)$ is outside of $[-L,L]$ can be derived similarly and more easily. Like the fuzzy PI controllers in the previous sections, the four fuzzy PI controllers in the present section become a linear P, I, or constant controller in the regions other than IC1 to IC4.

3.9.3. Characteristics of Gain Variation

We now study the properties of these four nonlinear fuzzy PI controllers in relation to the linear PI controller. As before, one only needs to study the characteristics of $\beta(e,r)$ as it is equivalent to studying the dynamic proportional-gain and integral-gain. As shown in Section 3.8, $E(n)$ and $R(n)$ can usually be managed to stay inside $[-L,L]$ to take full advantage of the

TABLE 3.6 The Formulas for Computing the Shadow Areas of the Trapezoidal Output Fuzzy Sets for the Four Different Inference Methods.

Inference Method	Formula for Computing the Shadow Area of the Trapezoidal Output Fuzzy Sets
R_M	$S_M(\mu) = \mu(2 - \mu + \mu\theta)H$
R_L	$S_L(\mu) = \mu(1 + \theta)H$
R_{DP}	$S_{DP}(\mu) = 2\mu\theta H$
R_{BP}	$S_{BP}(\mu) = \mu(2\theta + \mu - \mu\theta)H$

TABLE 3.7 The Expressions of $\beta(e, r)$ for the Four Different Inference Methods When Both $E(n)$ and $R(n)$ Are Within the Interval $[-L,L]$ (i.e., in IC1 to IC4—see Fig. 3.3).

$$\beta^M(e,r) = \frac{(3+\theta)L}{1+\theta} \times \frac{(1+\theta)L + 0.5(1-\theta)|K_e e(nT) - K_r r(nT)|}{(3+\theta)L^2 - [(1+\theta)L \cdot X(n) + 0.5(1-\theta)((K_e e(nT))^2 + (K_r r(nT))^2)]}$$

$$\beta^L(e,r) = \frac{2L}{2L - X(n)}$$

$$\beta^{DP}(e,r) = \frac{2L}{2L - X(n)}$$

$$\beta^{BP}(e,r) = \frac{(1+3\theta)L}{1+\theta} \times \frac{(1+\theta)L - 0.5(1-\theta)|K_e e(nT) - K_r r(nT)|}{(1+3\theta)L^2 - [(1+\theta)L \cdot X(n) - 0.5(1-\theta)((K_e e(nT))^2 + (K_r r(nT))^2]}$$

Note: $X(n) = \begin{cases} K_e|e(nT)|, & \text{IC1 and IC3} \\ K_r|r(nT)|, & \text{IC2 and IC4} \end{cases}$

TABLE 3.8 The Expressions of $K_p(0, 0)$ and $K_i(0, 0)$ for the Four Different Inference Methods When Both $E(n)$ and $R(n)$ Are Within the Interval $[-L,L]$ (i.e., IC1 to IC4).

Inference Method	$\frac{K_p(0,0)}{K_r}$ or $\frac{K_i(0,0)}{K_e}$
R_M	$\frac{(1+\theta)K_{\Delta u}H}{2(3+\theta)L}$
R_L	$\frac{K_{\Delta u}H}{4L}$
R_{DP}	$\frac{K_{\Delta u}H}{4L}$
R_{BP}	$\frac{(1+\theta)K_{\Delta u}H}{2(1+3\theta)L}$

gain variation, which means IC1 to IC4 are of the most importance and interest from a control standpoint. Therefore, in what follows, we will only analyze the characteristics of the fuzzy PI controllers when both $E(n)$ and $R(n)$ are inside $[-L,L]$.

$\beta^M(e,r)$, $\beta^L(e,r)$, $\beta^{DP}(e,r)$, and $\beta^{BP}(e,r)$ have the following properties:

$$\beta(e,r) = \beta(r,e) \tag{3.19}$$

$$\beta(e,r) = \beta(-r,-e). \tag{3.20}$$

Expression (3.19) indicates that all four $\beta(e,r)$ are symmetrical about the line

$$K_e e(n) = K_r r(n),$$

whereas (3.20) signifies the symmetry with respect to the line

$$K_e e(n) = -K_r r(n).$$

Because of the symmetries, it is sufficient to study $\beta(e,r)$ in one of the four ICs. Without losing generality, we choose IC1.

We begin with $\beta^M(e,r)$. It reaches its maximum when

$$K_e e(n) = L \quad \text{and} \quad K_r r(n) = -L$$

because the numerator of $\beta^M(e,r)$ becomes maximal while the denominator becomes minimal. The maximum of $\beta^M(e,r)$ is

$$\beta^M_{\max} = \frac{2(3+\theta)}{(1+\theta)^2}.$$

$\beta^M(e,r)$ attains its minimum when $e(n) = r(n) = 0$ because the numerator of $\beta^M(e,r)$ becomes minimal while the denominator becomes maximal. The minimum of $\beta^M(e,r)$ is 1. The ratio of $\beta^M_{\max}$ to $\beta^M_{\min}$ is

$$\rho^M = \frac{\beta^M_{\max}}{\beta^M_{\min}} = \frac{2(3+\theta)}{(1+\theta)^2}$$

which strictly monotonically decreases as θ increases from 0 to 0.5. The range of ρ^M is

$$\frac{28}{9} \le \rho^M \le 6$$

with maximal ρ^M at $\theta = 0$.

In IC1, $K_e e(n) \ge K_r r(n)$. For a given $K_r r(n)$, increase of $K_e e(n)$ makes the numerator of $\beta^M(e,r)$ larger and the denominator smaller, causing $\beta^M(e,r)$ to increase. For a given $K_e e(n)$, increase of $K_r r(n)$ also causes $\beta^M(e,r)$ to increase. When $K_e e(n) = L$ and $K_r r(n) = L$, $\beta^M(e,r)$ becomes

$$\beta^M_{L,L} = \frac{3+\theta}{1+\theta}.$$

On the basis of the properties of $\beta^M(e,r)$ in IC1 and the symmetries described in (3.19) and (3.20), we conclude that starting from the minimum at $K_e e(n) = 0$ and $K_r r(n) = 0$, $\beta^M(e,r)$ strictly monotonically increases with an increase of $K_e|e(n)|$ and $K_r|r(n)|$ in all directions. To visually confirm all these characteristics, a three-dimensional plot of $\beta^M(e,r)$ for $\theta = 0$ is demonstrated in Fig. 3.16.

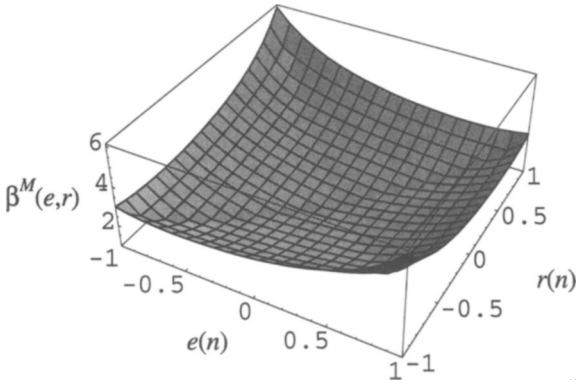

Figure 3.16 A three-dimensional plot of $\beta^M(e, r)$ for visualizing its properties analyzed in the text. For the plot, $\theta = 0$, $K_e = K_r = K_{\Delta u} = L = H = 1$. It can be seen that starting from the minimum at $K_e e(n) = 0$ and $K_r r(n) = 0$, $\beta^M(e,r)$ strictly monotonically increases with an increase of $K_e|e(n)|$ and $K_r|r(n)|$ in all directions. $\beta^M(e,r)$ achieves its maximum at $(L,-L)$ and $(-L,L)$.

We now study the properties of $\beta^L(e,r)$ and $\beta^{DP}(e,r)$. Because $\beta^L(e,r) = \beta^{DP}(e,r)$, the structure of the fuzzy controllers is identical and is independent of θ. When

$$K_e|e(n)| = L \quad \text{or} \quad K_r|r(n)| = L,$$

$\beta^L(e,r)$ and $\beta^{DP}(e,r)$ reach their maximum

$$\beta^L_{\max} = \beta^{DP}_{\max} = 2$$

and when

$$K_e e(n) = K_r r(n) = 0,$$

$\beta^L(e,r)$ and $\beta^{DP}(e,r)$ attain their minimum

$$\beta^L_{\min} = \beta^{DP}_{\min} = 1.$$

Therefore,

$$\rho^L = \rho^{DP} = \frac{\beta^L_{\max}}{\beta^L_{\min}} = \frac{\beta^{DP}_{\max}}{\beta^{DP}_{\min}} \equiv 2.$$

When $K_e e(n) = L$ and $K_r r(n) = L$, $\beta^L(e,r)$ and $\beta^{DP}(e,r)$ become

$$\beta^L_{LL} = \beta^{DP}_{LL} = 2.$$

In addition to being symmetrical about the lines (3.19) and (3.20), $\beta^L(e,r)$ and $\beta^{DP}(e,r)$ are also symmetrical about the lines

$$K_e e(n) = 0 \quad \text{and} \quad K_r r(n) = 0.$$

On the basis of the analyses, it can be concluded that starting from the minimum at $K_e e(n) = 0$ and $K_r r(n) = 0$, $\beta^L(e,r)$ and $\beta^{DP}(e,r)$ strictly monotonically increase with an increase of $K_e|e(n)|$ and $K_r|r(n)|$ in all directions. A three-dimensional plot of $\beta^L(e,r)$ (i.e., $\beta^{DP}(e,r)$) is demonstrated in Fig. 3.17.

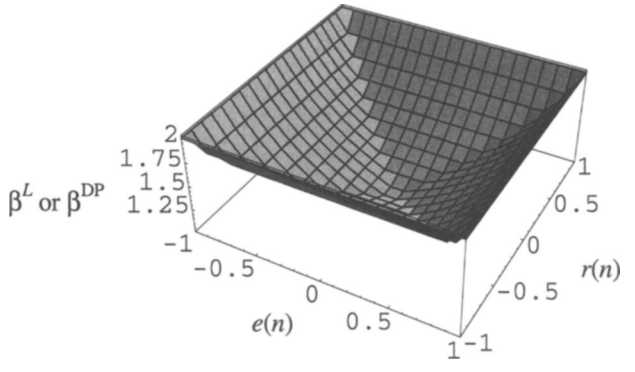

Figure 3.17 A three-dimensional plot of $\beta^L(e,r)$ and $\beta^{DP}(e,r)$ for visualizing their properties analyzed in the text. For the plot, $\theta = 0$, $K_e = K_r = K_{\Delta u} = L = H = 1$. It can be seen that starting from the minimum at $K_e e(n) = 0$ and $K_r r(n) = 0$, $\beta^M(e,r)$ strictly monotonically increases with an increase of $K_e|e(n)|$ and $K_r|r(n)|$ in all directions. $\beta^L(e,r)$ and $\beta^{DP}(e,r)$ achieves their maximum when $K_e|e(n)| = L$ and $K_r|r(n)| = L$.

3.9.4. Performance Enhancement by Gain Variation

We now look at the gain variation of the fuzzy PI controllers using R_M, R_L, and R_{DP} in the context of control. When $|E(n)|$ and $|R(n)|$ are larger, the fuzzy controllers issue relatively stronger control actions, owing mainly to larger $\beta^M(e,r)$, $\beta^L(e,r)$, and $\beta^{DP}(e,r)$. The maximal control actions occur when $K_e|e(n)| = L$ and/or $K_r|r(n)| = L$. The stronger control actions quickly reduce $e(n)$. On the other hand, when $|E(n)|$ and $|R(n)|$ are smaller, the fuzzy controllers call for relatively weaker control actions because of smaller $\beta^M(e,r)$, $\beta^L(e,r)$ and $\beta^{DP}(e,r)$. Minimal control actions take place when $K_e e(n) = 0$ and $K_r r(n) = 0$. The weaker control actions help gradually force system output to the setpoint in a manner that stabilizes the fuzzy control systems. From the control point of view, these behaviors of the fuzzy controllers are appropriate and desirable.

3.9.5. Unreasonable Gain Variation Characteristics Produced by Bounded Product Inference Method

We have purposely left $\beta^{BP}(e,r)$ unexamined so far because it does not possess desirable gain variation characteristics in the context of control. Note that when $K_e e(n) = L$ and $K_r r(n) = L$,

$$\beta^{BP}_{LL} = \frac{1+3\theta}{1+\theta}.$$

Furthermore, for different θ values, $\beta^{BP}(e,r)$ reaches different minima. It reaches

$$\beta^{BP}_{\min} = 1 \tag{3.21}$$

when $K_e e(n) = K_r r(n) = 0$, or it reaches

$$\beta^{BP}_{\min} = \frac{2\theta(1+3\theta)}{(1+\theta)^2} \tag{3.22}$$

when $K_e e(n) = L$ and $K_r r(n) = -L$. Let the right side of (3.21) equal the right side of (3.22) and solve the resulting equation for θ. The solution is

$$\theta = \frac{\sqrt{5}}{5} \approx 0.4472,$$

which means that when $0 \le \theta \le \sqrt{5}/5$, $\beta^{BP}(e,r)$ reaches the minimum in (3.22) and when $\sqrt{5}/5 \le \theta \le 0.5$, $\beta^{BP}(e,r)$ reaches the minimum in (3.21). It is easy to prove that when

$$0 \le \theta \le 0.1827,$$

a variable $\beta^{BP}_{\max}$ takes place at

$$(K_e e(n), K_r r(n)) = \left(\frac{3+3\theta-\sqrt{-13\theta^2+6\theta+3}}{2(1-\theta)} L, \frac{\sqrt{-13\theta^2+6\theta+3}-1-\theta}{2(1-\theta)} L \right),$$

which strictly monotonically increases from $(0.6340L, 0.3660L)$ at $\theta = 0$ to $(L, 0.4472L)$ at $\theta = 0.1827$. For the remaining values,

$$0.1827 \leq \theta \leq 0.5,$$

another variable $\beta_{\max}^{BP}$ occurs at

$$(K_e e(n), K_r r(n)) = \left(L, \left(3 + \frac{\sqrt{6\theta^2 + 8\theta + 2} - 4}{1 - \theta}\right)L\right)$$

which strictly monotonically increases from $(L, 0.4472L)$ at $\theta = 0.1827$ to $(L, 0.4772L)$ at $\theta = 0.5$. Because R_{BP} is inappropriate for control purposes, the exact expressions of $\beta_{\max}^{BP}$ and ρ^{BP} are unimportant and are omitted here. To visualize these theoretical discussions, two three-dimensional plots of $\beta^{BP}(e,r)$ for $\theta = 0$ and $\theta = 0.5$ are shown in Figs. 3.18a and b, respectively.

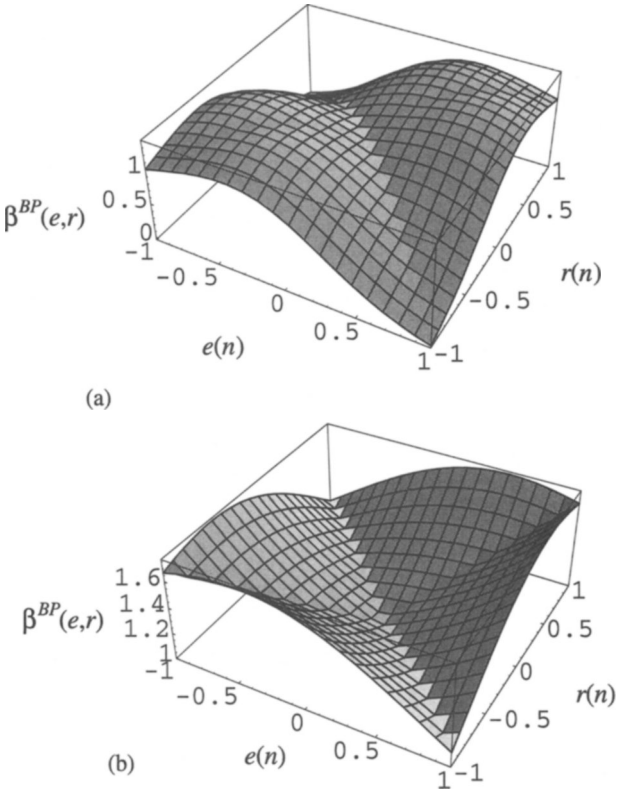

Figure 3.18 A three-dimensional plot of $\beta^{BP}(e, r)$ for visualizing its properties analyzed in the text. For the plot, $K_e = K_r = K_{\Delta u} = L = H = 1$. (a) $\theta = 0$. $\beta_{\min}^{BP}$ happens at $(L,-L)$ and $(-L,L)$, and $\beta_{\max}^{BP}$ takes place at $(0.634L, 0.366L)$, $(0.366L, 0.634L)$, $(-0.634L, -0.366L)$, and $(-0.366L, -0.634L)$. (b) $\theta = 0.5$. $\beta_{\min}^{BP}$ happens at $(0, 0)$, and $\beta_{\max}^{BP}$ takes place at $(L, 0.4772L)$, $(0.4772L, L)$, $(-L, -0.4772L)$, and $(-0.4772L, -L)$.

Unlike $\beta_{\max}^{M}$, $\beta_{\max}^{L}$, and $\beta_{\max}^{DP}$, $\beta_{\max}^{BP}$ does not occur when $K_e|e(n)| = L$ and/or $K_r|r(n)| = L$. This implies that the fuzzy controller using R_{BP} sometimes takes relatively strong action when the absolute values of the scaled inputs are small and relatively weak action when the absolute values of the scaled inputs are large. In other words, the magnitude of the control action is not always consistent with respect to the magnitude of the inputs. The inconsistency is generally insensible and inappropriate from the control point of view. In addition, the occurrence of $\beta_{\min}^{BP}$ at $(L,-L)$ and $(-L,L)$ is undesirable. Thus, R_{BP} is not a reasonable inference method for fuzzy control.

3.9.6. Conclusion on Fuzzy Inference Methods for Control

A few years before the above results were obtained, comparison results of 12 different fuzzy inference methods, including the four described here, were reported in the literature [157]. The other eight inference methods include the standard sequence method, the Gödelian logic method, and the Gougen method. The comparison was not conducted theoretically; rather, it was carried out using computer simulation and a first order with a time-delay model. Configurations of the fuzzy controllers differed from those of the fuzzy PI controllers here. According to the simulation results, the fuzzy controllers using R_M, R_L, R_{DP}, and R_{BP} produced much better results than the fuzzy controllers using the other inference methods. Through rigorous mathematical analysis, we can now conclude that R_{BP} is inappropriate. Therefore, only 3 of the 12 inference methods are suitable for fuzzy control.

3.10. SIMPLEST TITO FUZZY PI CONTROLLER AS TITO NONLINEAR VARIABLE GAIN PI CONTROLLER

3.10.1. Fuzzy Controller Configuration

We now extend SISO fuzzy PI control to a TITO (two-input two-output) case. The TITO fuzzy PI controller, shown in Fig. 3.19, uses four input variables:

$$E_1(n) = K_e^1 \cdot e_1(n) = K_e^1(S_1(n) - y_1(n)) \tag{3.23}$$

$$R_1(n) = K_r^1 \cdot r_1(n) = K_r^1(e_1(n) - e_1(n-1)) \tag{3.24}$$

$$E_2(n) = K_e^2 \cdot e_2(n) = K_e^2(S_2(n) - y_2(n)) \tag{3.25}$$

$$R_2(n) = K_r^2 \cdot r_2(n) = K_r^2(e_2(n) - e_2(n-1)) \tag{3.26}$$

where K_e^1, K_e^2, K_r^1, and K_r^2 are scaling factors, and $y_1(n)$ and $y_2(n)$ are coupling outputs of a TITO system with respective setpoints, $S_1(n)$ and $S_2(n)$. Each scaled variable is fuzzified by two fuzzy sets, Positive and Negative. For notations, we use $\tilde{A}_{i,1}$ and $\tilde{A}_{i,-1}$ to represent Positive and Negative fuzzy sets for $E_i(n)$, respectively. The same fuzzy sets are represented by $\tilde{B}_{i,1}$ and $\tilde{B}_{i,-1}$ for $R_i(n)$. The shapes of the membership functions are identical to those shown in Fig.